Lubricant-infused micro/nano-structured surfaces with tunable dynamic omniphobicity at high temperatures

Lubricant-Infused Micro/Nano-structured Surfaces with Tunable Dynamic Omniphobicity at High Temperatures

Daniel Daniel,[1,a)] Max N. Mankin,[2,a)] Rebecca A. Belisle,[3] Tak-Sing Wong,[1,3,b),c)] and Joanna Aizenberg[1,2,3,c)]

[1]School of Engineering and Applied Sciences, Harvard University, Cambridge, MA 02138

[2]Department of Chemistry and Chemical Biology, Harvard University, Cambridge, MA 02138

[3]Wyss Institute for Biologically Inspired Engineering, Harvard University, Cambridge, MA 02138

Omniphobic surfaces that can repel fluids at temperatures higher than 100°C are rare. Most state-of-the-art liquid-repellent materials are based on the lotus effect, where a thin air layer is maintained throughout micro/nanotextures leading to high mobility of liquids. However, such behavior eventually fails at elevated temperatures when the surface tension of test liquids decreases significantly. Here, we demonstrate a class of lubricant-infused structured surfaces that can maintain a robust omniphobic state even for low-surface-tension liquids at temperatures up to at least 200°C. We also demonstrate how liquid mobility on such surfaces can be tuned by a factor of 1000.

The ability of surfaces to repel various liquids (i.e. omniphobicity) at elevated temperatures have broad practical applications in refinery processes, ethanol concentration, fuel transportation, district heating, and protective fabrics.[1,2] State-of-the-art approaches have

[a] D. Daniel and M.N. Mankin contributed equally to this work

[b] Present Address: Department of Mechanical and Nuclear Engineering, The Pennsylvania State University, PA 16802

[c] Authors to whom correspondence should be addressed. Electronic mail: tswong@psu.edu and jaiz@seas.harvard.edu

been based on the 'lotus' effect, where micro/nano-structures are carefully designed to maintain an air layer between the structures, forming a stable interface between the substrate and the applied liquid.[3,4] This superhydrophobic interface, however, becomes unstable for low-surface-tension liquids due to their enhanced ability to wet surfaces.[5] Since surface tension decreases with increasing temperature – which further destabilizes the liquid-air interface – it is very challenging to design surfaces that can repel a wide range of liquids at high temperatures.

Early work on omniphobicity employed photolithography to create complex re-entry geometries on a surface, which could then repel liquids with surface tension down to ~17 mN/m (e.g. heptane) at ambient temperature.[6,7] Other approaches to generating re-entry geometries that achieve omniphobicity were later demonstrated.[8-10] It was also shown that small liquid droplets can bounce off an extremely hot superhydrophobic surface reminiscent of the Leidenfrost effect, provided that the heat transfer between the solid and liquid is sufficient to generate a vapor layer, which can only occur when the temperature of the solid substrate T_{solid} is significantly above the liquid's boiling point (T_{solid} > 150°C for water).[11] Recent progress in creating superhydrophobic/superoleophobic materials based on fluorinated silica network and rare-earth oxide ceramics addressed the problem of developing mechanically robust surfaces that retain liquid-repellency (quantified by contact angle at *ambient* temperature), after annealing/sintering of the substrate at high temperatures up to 1000°C.[12-14] While these surfaces have high-temperature stability during their respective manufacturing processes and remain liquid-repellent after cooling down to room temperature, they did not demonstrate liquid repellency at elevated temperatures. Oleophobic surface based on polymethylsilsesquioxane coating, on the other hand, has been shown to repel organic liquids at 250°C.[15] Nonetheless, omniphobic surfaces that can repel various fluids at elevated temperatures (when either T_{liquid} or T_{solid} or both are above 200°C) remain rare, due

to the fact that surface tensions of some organic liquids, such as heptane and octane, can fall below 10 mN/m at $T > 200°C$.[16,17]

Recently, we developed a radically different concept in designing omniphobic surfaces, termed as Slippery Liquid-Infused Porous Surfaces (SLIPS) in which a suitably treated micro/nano-structured surface is infused with a lubricating fluid, as shown in Fig. 1a. Any foreign liquid droplet immiscible with the underlying lubricating fluid can then easily slide off at a small tilting angle of $< 5°$.[18] We demonstrated how such a principle can be applied to a variety of solid substrates, including polymers, metals, glass and ceramics, such that arbitrary materials begin to show superior liquid-repellency, anti-biofouling, and anti-icing properties.[19-21] Lafuma and Quéré outlined the requirements for thermodynamic stability for such a system, which was further elaborated by Smith et al.[22,23] Here, we report that SLIPS retain their excellent liquid-repelling properties at high temperatures up to $T_{solid,liquid} = 200°C$ for a wide range of liquids, including those with low surface tension. This is in contrast with the best superhydrophobic (SH) surfaces that were shown to lose their liquid-repellency even at moderate $T_{liquid} \sim 90°C$.[1]

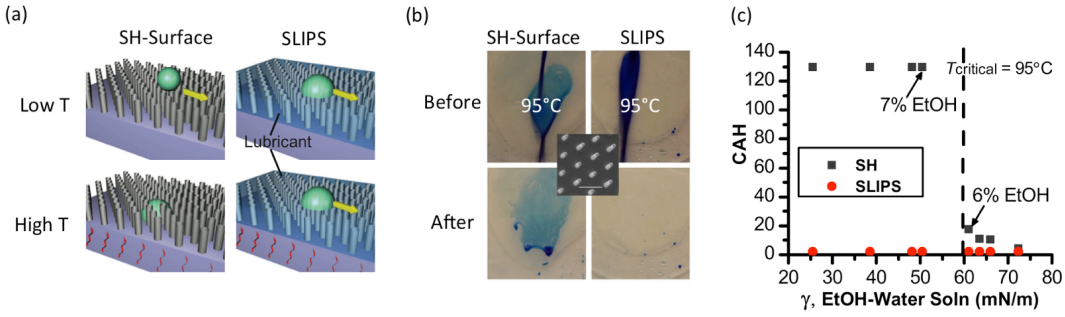

FIG. 1. (a) Schematic of superhydrophobic (SH-) surface (Left) and SLIPS (Right): In SH-surface, there is a transition from non-wetting to wetting with increase in T. SLIPS on the other hand remain liquid-repellent at high T. (b) Hot water (T = 95°C) stained with methylene blue effectively wets SH-surface, while the same surface infused with Krytox 100 remains dry and stain-free. (Enhanced Online) [URL: Movie 1] (c) Plot shows the CAH on SH-surface (black squares) and SLIPS (red circles) for water and water-EtOH solutions of increasing concentrations of EtOH (2, 5, 6, 7, 10 and 20% wt).

SLIPS can be created from a SH-surface by infusing it with a lubricant such as perfluorinated oil. A micro-structured surface consisting of a hexagonal array of posts with dimensions d = 1 μm, height h = 10 μm, and pitch l = 4 μm, illustrated in inset of Fig. 1b, was fabricated using fast replication techniques described elsewhere.[24] The final substrate was made of UV-cured polyurethane (NOA 61, Norland) which was then fluorinated to render its surfaces SH. At room temperature, this SH-surface repels water with a contact angle of 165±5°, but when 200 mL of hot water (T_{liquid} = 95°C, stained with methylene blue) was splashed onto the surface, the surface was clearly wetted, as shown in Fig. 1b. The same solid substrate infused with perfluorinated polyethers (Krytox 100, DuPont, lubricant thickness = 13 μm) retained its water-repellency even at 95°C.

To confirm that the decrease in surface tension, γ, was the cause of the transition from a non-wetting to a wetting state, we measured the contact angle hysteresis (CAH) for water-ethanol mixtures of increasing ethanol (EtOH) concentration (0-70% wt) on the SH-surface and SLIPS to simulate the effect of water surface tension drop due to increasing temperature, T_{liquid}, as summarized in Fig. 1c. Near boiling, water has surface tension of 58 mN/m as opposed to its room temperature value of 72.8 mN/m.[25] For SLIPS, CAH remained small (~2°) for all EtOH concentrations, whereas for the SH-surface, there was a transition from non-wetting to wetting when the liquid droplet reached a critical surface tension, $50 < \gamma_{critical} < 60$ mN/m. The CAH for 6% EtOH was 18°, whereas for 7% EtOH, the receding contact angle was ~0° while the advancing contact angle was 130°, i.e. CAH = 130°. This sharp pinning transition is consistent with the wetting observed for water at T_{liquid} = 95°C, where γ_{water} = 59.8 mN/m approaches $\gamma_{6\%EtOH}$, shown as a dashed line in Fig. 1c. Similar wetting temperature, $T_{wetting} = 94 \pm 1°$, was observed for a SH-surface dipped in hot water for 1 min to ensure that the surface and water were at the same temperature, i.e. $T_{solid} = T_{liquid}$.

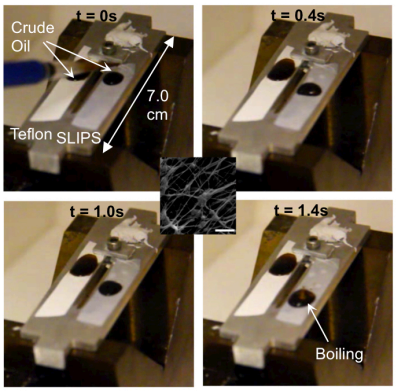

FIG. 2. Images at time t = 0-1.4s of two 50 µL crude oil droplets on 10° incline placed next to each other on a hot plate, one pinned to a Teflon membrane and the other sliding at a speed of 1.5 cm/s on the same membrane infused with Krytox 105. At t = 1.4 s, crude oil started to boil. Inset: SEM of the Teflon membrane (scale bar 1 µm). (Enhanced Online) [URL: Movie 2]

While these surfaces show promise in applications that involve high-temperature water transport and heating, it is unsuitable for ultra-high temperature applications involving liquids with high boiling point, since Norland 61 polymer begins to degrade at T_{solid} ~ 150°C. To investigate the effects of T > 100°C, a Teflon membrane (pore size ~0.2µm, thickness ~50µm), which resists degradation up to 350°C, was chosen as the solid substrate. Fig. 2 demonstrates that a Teflon membrane infused with perfluorinated Krytox 105 easily repels a 50 µL droplet of crude oil at T_{SLIPS} = 200°C. Even at a small incline of 10°, the droplet moved at a speed of ~1.5 cm/s, whereas the crude oil droplet on the bare Teflon membrane (SH state) was pinned to the surface. The crude oil used contained mostly light oil fractions with a boiling temperature of around 150°C. SLIPS remained liquid-repellent even when the crude oil droplet started to boil. At T = 200°C, crude oil is known to have a surface tension <20 mN/m.[26,27]

It is important to note that liquid-repellency of the material is associated with and can be described in terms of how quickly liquid droplets can move on and hence be removed from the surface. This in turn is significantly affected by the viscosity of the lubricating layer, $\eta_{lubricant}$, since the viscous force associated with the trapped lubricating film scales linearly with $\eta_{lubricant}$.[23,28,29] Unlike SH-surface, liquid droplets on SLIPS will therefore become more mobile with initial increase in temperature, as $\eta_{lubricant}$ drops with increasing temperature. We measured the velocity of 20 µL droplets of crude oil moving on a heated Teflon membrane infused with various lubricants (perfluorinated polyethers, DuPont Krytox 100, 103, 105 with

chain length n = 10-60, that have similar surface tensions of γ = 17±1 mN/m but different viscosities $\eta_{101,103,105}$ = 20, 140, 800 cP at room temperature) and positioned at small 5° tilt angle at temperatures T_{SLIPS} = 20-200°C. The results are summarized in Fig. 3. Each measurement was repeated 3-5 times and a thermocouple was used to monitor the temperature of the surface. For each case, the velocity of the droplet, V, first increases with T, as shown in Fig. 3a, because the viscosity of Krytox oils decreases with increasing T_{SLIPS}, illustrated in Fig. 3b, but only up to a critical temperature, T_c. With further heating beyond T_c, the Krytox oil evaporation rate becomes significant and the velocity of the droplets decreases due to pinning at exposed defects on SLIPS. T_c was observed to increase with Krytox oils index, because higher-index Krytox oils contain longer-chain polyethers. Fig. 3c shows the results of thermogravimetric analysis, which confirms that the higher-index Krytox oils evaporate at higher T_{SLIPS}, with maximum rate of evaporation occurring at T_{max} = 170, 269, and 395°C for Krytox 100, 103 and 105, respectively. Inferring T_c directly from the thermogravimetric data is not trivial and it was found that T_c occurs well below T_{max}. Nevertheless, the values of T_c for the different Krytox oils obtained, $T_{c,100} \approx 70$°C, $T_{c,103} \approx 100$°C, $T_{c,105} > 150$°C are consistent with the maximum operating temperature T, shown by dashed lines in Fig. 3a, provided by the manufacturer.

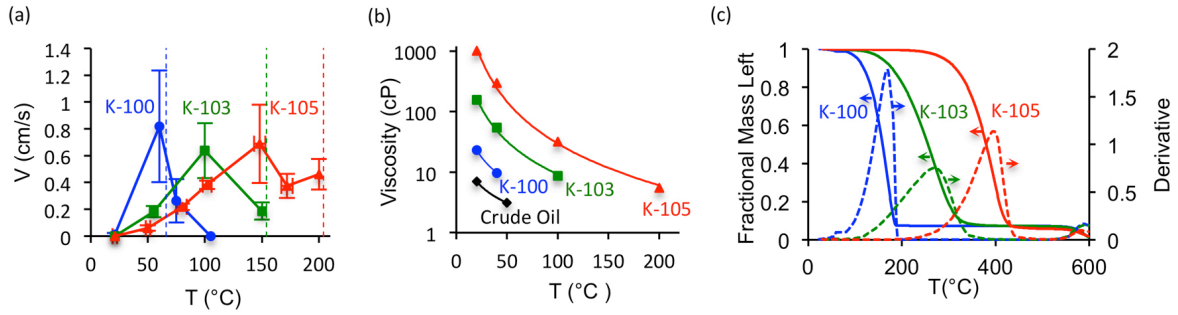

FIG. 3. Characterization of lubricant viscosity and stability at high temperatures and the resulting velocity of the moving liquid droplets. (a) Velocities of 20 µL droplets of crude oil moving down a Teflon membrane infused with perfluorinated Krytox oils 100, 103 and 105 (K-100, 103 and 105) inclined at 5° for temperatures T = 20-200°C. Vertical dashed lines denote to the maximum operating temperature for the different Krytox oils. (b) Viscosities of the corresponding Krytox oils, η_{100}, η_{103} and η_{105} as a function of increasing T. For a fixed T, $\eta_{105} \approx 10\ \eta_{103} \approx 100\ \eta_{100}$. (c) Thermogravimetric analysis of Krytox oils demonstrates that the rate of evaporation peaks at increasing T for higher index number. Solid lines represent fractional mass left, while dashed lines represent the rate of fractional mass loss.

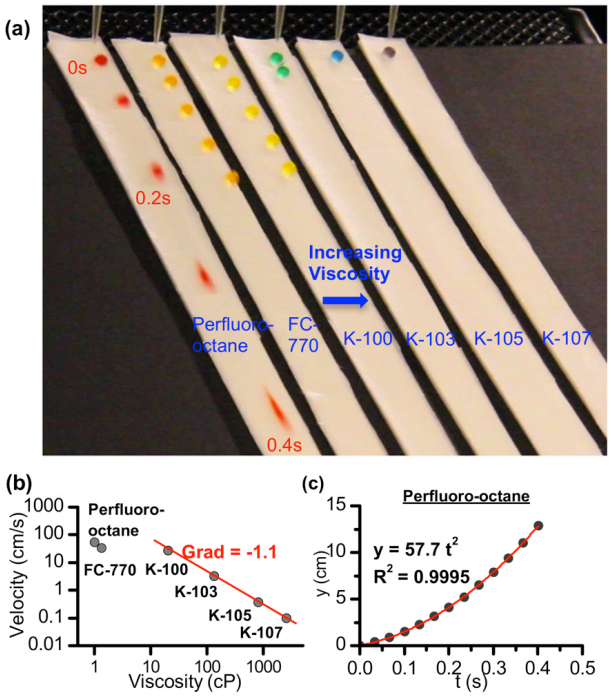

FIG. 4. (a) Time-lapsed image (total time lag Δt = 0.4s) of 20 μL water droplets down a 50° incline for Teflon membrane infused with lubricants with increasing viscosity: (left to right) perfluoro-octane, FC-770, Krytox-es 100, 103, 105 and 107. (Enhanced Online) [URL: Movie 3] (b) Log-log plot showing dependence of droplet velocity on lubricant viscosity. (c) Distance traveled by the water droplet with time on perfluoro-octane-infused surface. Water did not reach terminal velocity and instead accelerated at constant a = 1.15 m/s^2.

To further demonstrate the effects of $\eta_{\text{lubricant}}$ on the mobility of liquid droplets, we measured the velocity of 20 μL water droplets down an incline of 50° for Teflon membranes infused with perfluorinated liquids (perfluoro-octane, FC-770, Krytox 100-107) of increasing viscosity, $\eta_{\text{lubricant}}$ = 1-2500 cP. Fig. 4a shows a time-lapsed image of such an experiment, in which the positions of differently colored water droplets at equally spaced time intervals are juxtaposed. Each 30 cm lane was infused with different lubricants (increasing $\eta_{\text{lubricant}}$ from left to right) and the time-lag, Δt, from start to finish is 0.4 s. Fig. 4b shows a log-log plot of the velocity of water droplets and the viscosity of lubricant. For the most viscous lubricant, Krytox 107, which is ~2500 times more viscous than water, the droplet moved at a speed of about 1 mm/s, whereas for perfluoro-octane, which is as viscous as water ($\eta_{\text{lubricant}}$ ~ 1cP), the maximum velocity at the end of the 30cm track reached an extremely high value of ~0.5 m/s. To put this into perspective, a similarly sized water droplet moves down a vertically inclined glass at a speed of ~1 cm/s. In Fig. 4c, the plot of the droplet displacement on perfluoroctane-

infused surface with time shows a quadratic relationship, i.e. the droplet was accelerating at a constant a = 1.15 m/s^2, c.f. g sin(50°) = 7.5 m/s^2. The discrepancy between the gravitational acceleration g sin(50°), and the observed acceleration, a, is probably due to friction between the underlying solid substrate and the liquid droplet. For Teflon infused with other lubricants, the droplets achieved their terminal velocities.

The results of the experiments depicted in Figs 3 and 4 demonstrate that it is possible to tune the velocity of droplets on SLIPS continuously by a factor of 1000 on the same solid substrate by either 1) changing the temperature of the surface or 2) using lubricants of different viscosities. This capability has broader implications in terms of droplet manipulation on surfaces. In textured SH-surface, droplet mobility is dictated by the static contact angle θ_s and CAH, but the two parameters do not sufficiently characterize droplet behavior on SLIPS. The water droplets on different lubricant-infused SLIPS have similar θ_s = 115 ± 2° and CAH ~ 3°, but nevertheless travel at a wide range of velocities, showing the importance of the lubricant as an additional source of friction/resistance for the droplet movement. Our results also suggest that within different temperature regimes, there is an optimum lubricant that maximizes the velocity of droplet: Krytox 100 for T_{SLIPS} < 70°C, Krytox 103 for T_{SLIPS} =70-120°C, and Krytox 105 for T_{SLIPS} =120-200°C. We did not measure the mobility of crude oil droplets for T_{SLIPS} > 200°C for reasons of safety, but TGA analysis indicates that when infused with Krytox 105, SLIPS can retain its liquid-repellency up to T_{SLIPS} ~ 300°C, as depicted in Fig. 3c. The lifetime of SLIPS at high temperatures is closely related to the evaporation rate of the lubricant and therefore increases with increasing Krytox index. (See supplemental material for discussion of SLIPS lifetime)

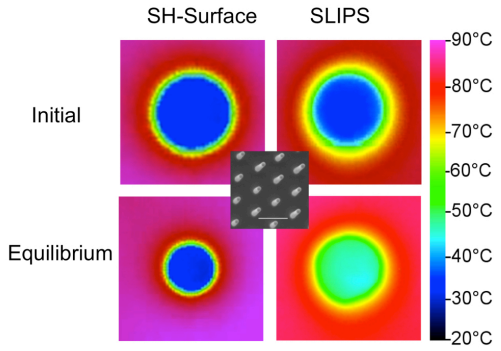

FIG. 5. Infra-red image of a 20 μL water droplet on a superhydrophobic surface (Left) and SLIPS (Right) taken normal to the surface. Inset: SEM of a solid substrate with an hexagonal array of posts (diameter d = 1 μm, height h = 10 μm and pitch l = 4 μm) used in the experiment. Scale bar 5 μm.

Finally, SLIPS exhibit a much better heat transfer rate than SH-surface and this may be relevant in some industrial processes where heat transfer is important.[30,31] 20 μL water droplets were placed on a lotus-surface and its SLIPS counterpart (same surfaces as Fig. 1) that were kept at a temperature $T_{solid} = 85 \pm 5°$ using a thermal plate. The temperatures of the water droplet and the surfaces were measured using an infrared camera, as shown in Fig. 5. Initially, both water droplets were at room temperature, but at equilibrium, the cores of the water droplets were at different temperatures: $T_{core,SLIPS} = 45 \pm 2° > T_{core,SH} = 32 \pm 2°$. The equilibrium temperatures, $T_{core,SLIPS}$ and $T_{core,SH}$ remained constant until all of the liquid droplets have completely evaporated. Potentially, this heat transfer rate can be further controlled by adjusting the thermal conductivity of the lubricants.

To summarize, we have demonstrated a system that is capable of repelling a wide range of liquids, from simple newtonian fluid such as water to a low-surface-tension complex fluid such as crude oil, across a wide range of temperatures up to 200°C. In comparison, most state-of-the-art SH-surfaces fail at moderate $T < 90°C$. We also outlined how to manipulate droplet's mobility on SLIPS continuouly on the same solid surface by a factor of 1000 by either changing the temperature or using different lubricants. We believe that such a tunable, robust omniphobic surfaces will have many uses in industrial processes that involve liquid manipulation and transport in challenging, high temperature conditions.

We thank P. Kim for helpful discussions regarding TGA. M.N.M. gratefully acknowledges a Fannie and John Hertz Foundation Graduate Fellowship and a NSF Graduate

Research Fellowship. The work was supported partially by the ONR MURI award #N00014-12-1-0875 and ARPA-E award. We acknowledge the use of the facilities at the Harvard Center for Nanoscale Systems supported by the NSF under award ECS-0335765.

REFERENCES

[1] Y. Liu, X. Chen, and J.H. Xin, J. Mater. Chem. **19**, 5602 (2009).

[2] G.Y. Lai, *High-Temperature Corrosion and Materials Applications* (ASM International, Ohio, 2007) pp 321-334.

[3] D. Quéré, Annu. Rev. Mater. Res. **38**, 71 (2008).

[4] L. Bocquet and E. Lauga, Nature **10**, 334 (2011).

[5] E.G. Shafrin and W.A. Zisman, *Constitutive Relations in the Wetting of Low-Energy Surfaces and the Theory of Retraction Method of Preparing Monolayers* (Naval Research Lab., Washington D.C., 1959).

[6] A. Tuteja, W. Choi, J.M. Mabry, G.H. McKinley, and R.E. Cohen, Proc. Natl. Acad. Sci. USA **105**, 18200 (2008).

[7] A. Ahuja, J.A. Taylor, V. Lifton, A.A. Sidorenko, T.R. Salamon, E.J. Lobaton, P. Kolodner, and T.N. Krupenkin, Langmuir **24**, 9 (2008).

[8] H. Li, X. Wang, Y. Song, Y. Liu, Q. Li, L. Jiang, and D. Zhu, Angew. Chem. **40**, 1743 (2001).

[9] A. Grigoryev, I Tokarev, K.G. Kornev, I. Luzinov and S. Minko, J. Am. Chem. Soc. **134**, 12916 (2012).

[10] S. Peechok and B. Pokroy, Adv. Funct. Mater. **22**, 745-750 (2013).

[11] T. Zhang, J. Wang, L. Chen, J. Zhai, Y. Song, and L. Jiang, Angew. Chem. **50**, 5311 (2011).

[12] X. Deng, L. Hamman, H.-J. Butt, and D. Vollmer, Science, **335**, 67 (2011).

[13] M. Guo, B. Ding, X. Li, J. Yu, and M. Wang, J. Phys. Chem. C **114**, 916 (2010).

[14] G. Azimi, R. Dhiman, H.-M. Kwon, A.T. Paxson, and K.K. Varanasi, Nature Materials **12**, 1 (2013).

[15] C. Urata, B. Masheder, D.F. Cheng, and A. Hozumi, Chem. Commun. (2013). DOI:10.1039/C3CC41087K

[16] J.J. Jasper, J. Phys. Chem. Ref. Data **1**, 841 (1972).

[17] J. Escobedo and G.A. Mansoori, AICHE J. **42**, 1425 (1996).

[18] T.-S. Wong, S.H. Kang, S.K.Y. Tang, E.J. Smythe, B.D. Hatton, A. Grinthal, and J. Aizenberg, Nature **477**, 443 (2011)

[19] P. Kim, T.S. Wong, J. Alvarenga, M.J. Kreder, W.E. Ardono-Martinez, and J. Aizenberg, ACS Nano **6**, 6569 (2012).

[20] A.K. Epstein, T.S. Wong, R.A. Belisle, E.M. Boggs, and J. Aizenberg, Proc. Natl. Acad. Sci. USA **109**, 13133 (2012).

[21] P. Kim, M.J. Kreder, J. Alvarenga, and J. Aizenberg, Nano Lett. (2013).
DOI: 10.1021/nl4003969

[22] A. Lafuma and D. Quéré, Europhys. Lett. **96**, 56001 (2011).

[23] J.D. Smith, R. Dhiman, S. Anand, E. Reza-Garduno, R.E. Cohen, G.H. McKinley, and K.K. Varansi, Soft Matter **9**, 1772 (2013).

[24] B. Pokroy, A.K. Epstein, M.C.M. Persson-Gulda, and J. Aizenberg, Adv. Mater. **21**, 463 (2009).

[25] N.B. Vargaftik, N.B. Volkov, and L.D. Voljak, J. Phys. Chem. Ref. Data **12**, 817 (1963).

[26] G. Winchester and R.K. Reber, Ind. Eng. Chem. **21** 1093 (1929).

[27] S. Ross, *Variation with Temperature of Surface Tension of Lubricating Oils* (National Advisory Committee for Aeronautics, Washington, 1950).

[28] J. Seiwert, M. Maleki, C. Clanet, and D. Quéré, Europhys. Lett. **94**, 16002 (2011).

[29] J. Seiwart, M. Maleki, and D. Quéré, J. Fluid. Mech. **669**, 55 (2011).

[30] K.-Han. Chu, R. Enright, and E.N. Wang, Appl. Phys. Lett. **100**, 241603 (2012).

[31] N. Miljkovic, R. Enright, Y. Nam, K. Lopez, N. Dou, J. Sack, and E.N. Wang, Nano Lett. **13**, 179 (2013).